Morphology, Crystallization, and Thermal Behavior of Isotactic Polypropylene/Propylene-*g*-Styrene Blends

L. D'ORAZIO,[1] R. GUARINO,[1] C. MANCARELLA,[1] E. MARTUSCELLI,[1] G. CECCHIN[2]

[1] Istituto di Ricerca e Tecnologia delle Materie Plastiche del CNR Via Toiano, 6, 80072 Arco Felice, Napoli, Italy

[2] Montell Italia S.p.A, Ferrara, Italy

Received 20 March 2000; accepted 29 May 2000

ABSTRACT: Optical microscopy, differential scanning calorimetry, and small angle X-ray scattering techniques were used to study the influence of the crystallization conditions on morphology and thermal behavior of samples of binary blends constituted of isotactic polypropylene (iPP) and a novel graft copolymer of unsaturated propylene with styrene (uPP-*g*-PS) isothermally crystallized from melt, at relatively low undercooling, in a range of crystallization temperatures of the iPP phase. It was shown that, irrespective of composition, no fall in the crystallinity index of the iPP phase was observed. Notwithstanding, spherulitic texture and thermal behavior of the iPP phase in the iPP/uPP-*g*-PS materials were strongly modified by the presence of copolymer. Surprisingly, iPP spherulites crystallized from the blends showed size and regularity higher than that exhibited by plain iPP spherulites. Moreover, the amount of amorphous material located in the interspherulitic amorphous regions decreased with increasing crystallization temperature, and for a given crystallization temperature, with increasing uPP-*g*-PS content. Also, relevant thermodynamic parameters, related to the crystallization process of the iPP phase from iPP/uPP-*g*-PS melts, were found, composition dependent. The equilibrium melting temperature and the surface free energy of folding of the iPP lamellar crystals grown in the presence of uPP-*g*-PS content up to 5% (wt/wt) were, in fact, respectively slightly lower and higher than that found for the lamellar crystals of plain iPP. By further increase of the copolymer content, both the equilibrium melting temperature and surface free energy of folding values were, on the contrary, depressed dramatically. The obtained results were accounted for by assuming that the iPP crystallization process from iPP/uPP-*g*-PS melts could occur through molecular fractionation inducing a combination of morphological and thermodynamic effects.
 J Appl Polym Sci 79: 2286–2298, 2001

Key words: isotactic polypropylene; propylene-*g*-styrene; morphology; crystallization; blends

INTRODUCTION

A novel graft copolymer of unsaturated propylene with styrene (uPP-*g*-PS) has been added to isotactic polypropylene (iPP) to investigate the state of mixing between the uPP-*g*-PS and iPP phase and the effects of the uPP-*g*-PS addition on the iPP intrinsic phase structure, i.e., on the iPP spherulitic texture and inner structure of the spherulites fibrillae. In a previous article,[1] we reported results of an investigation performed on thin films of iPP/uPP-*g*-PS blends containing 2, 5, and 10%

Correspondence to: L. D'Orazio.

Journal of Applied Polymer Science, Vol. 79, 2286–2298 (2001)

Table I Molecular Characteristics of the Starting Polymers Together with Glass Transition Temperature (T_g), Apparent Melting Temperature (T'_m), and Crystallinity Index (X_c)

Sample	$\bar{M}_n$ (g/mol)	$\bar{M}_w$ (g/mol)	$\bar{M}_w/\bar{M}_n$	η (dl/g)	% PS (wt/wt)	T_g (°C)	T'_m (°C)	X_c
iPP	78,700	509,000	6.5	2.0	—	−9	168	0.52
uPP-*g*-PS	—	—	—	1.4	35	11 118	142	0.22

(wt/wt) of graft copolymer, obtained by *o*-dichlorobenzene casting, according to the method previously used to compatibilize samples of iPP/atactic polystyrene blends through the addition of the uPP-*g*-PS phase.[2,3] The variation of tangent δ with temperature and differential scanning calorimetry (DSC) thermograms of the iPP/uPP-*g*-PS binary systems showed respectively that, regardless of blend composition, a single glass transition temperature (T_g) and a single apparent melting temperature (T'_m) is found for the iPP phase. Optical microscopy (OM) investigation revealed that, with increasing uPP-*g*-PS content, iPP spherulites become more open and coarse, with both dimension and number per unit area of the amorphous interspherulitic contact regions decreasing. The long period (L) values of the iPP phase, calculated from the peak position of Lorentz-corrected desmeared small angle X-ray scattering (SAXS) profiles, increased markedly with increasing uPP-*g*-PS content; such an increase is due to an increase of both average crystalline lamellar thickness (L_c) and interlamellar amorphous phase (L_a).

In the present article, we report on results of an investigation aimed at establishing the influence of the crystallization conditions on morphology of phase and interphase developed after complete crystallization from the melt state under controlled crystallization conditions in film samples of iPP/uPP-*g*-PS blends isothermally crystallized, at relatively low undercooling, in a range of crystallization temperatures of the iPP phase. The combined effects of undercooling and composition on the kinetic and thermodynamic parameters related to the isothermal crystallization process of the iPP phase have also been investigated.

EXPERIMENTAL

Materials

The starting polymers used in this study were an iPP (HS005) made by Himont (Ferrara, Italy) and a uPP-*g*-PS copolymer synthesized in the Himont scientific laboratories according to methods patented by Cecchin et al.[4,5] from Himont. The molecular characteristics of the plain starting materials are reported in Table I together with their T_gs, T'_m, and crystallinity indices (X_c).

Blending and Sample Preparation

All of the investigated samples were obtained by means of the solvent casting method. The blend components were dissolved in a common solvent, *o*-dichlorobenzene, at a total polymer concentration of 3% by weight and at the temperature of 135°C. Thin films were then obtained by *o*-dichlorobenzene casting performed under vacuum at the temperature of 135°C for 3 h. iPP/uPP-*g*-PS binary blends containing 2, 5, and 10% (wt/wt) of graft copolymer were prepared.

Techniques

DSC

The thermal behavior of the thin films of plain iPP and its blends isothermally crystallized at the temperatures of 126, 130, 134, and 138°C, was analyzed by means of DSC with a Mettler TA 3000 instrument equipped with a control and programming unit (microprocessor Tc 10). The T'_m and the X_c were determined following this procedure: the film samples (about 9 mg), heated from room temperature up to 200°C with a rate of 10°C/min and kept at this temperature for 10 min to destroy any trace of crystallinity, were rapidly cooled to the desired T_c; after complete crystallization, such samples were again heated at 200°C with a rate of 10°C/min. The observed T'_m and the apparent enthalpies of melting (ΔH^*) were obtained from the maxima and the area of the melting peaks, respectively. The X_c of iPP and of blends were calculated by applying the following relations:

$$X_c(\text{iPP}) = \Delta H^*(\text{iPP})/\Delta H^0(\text{iPP}) \quad (1)$$

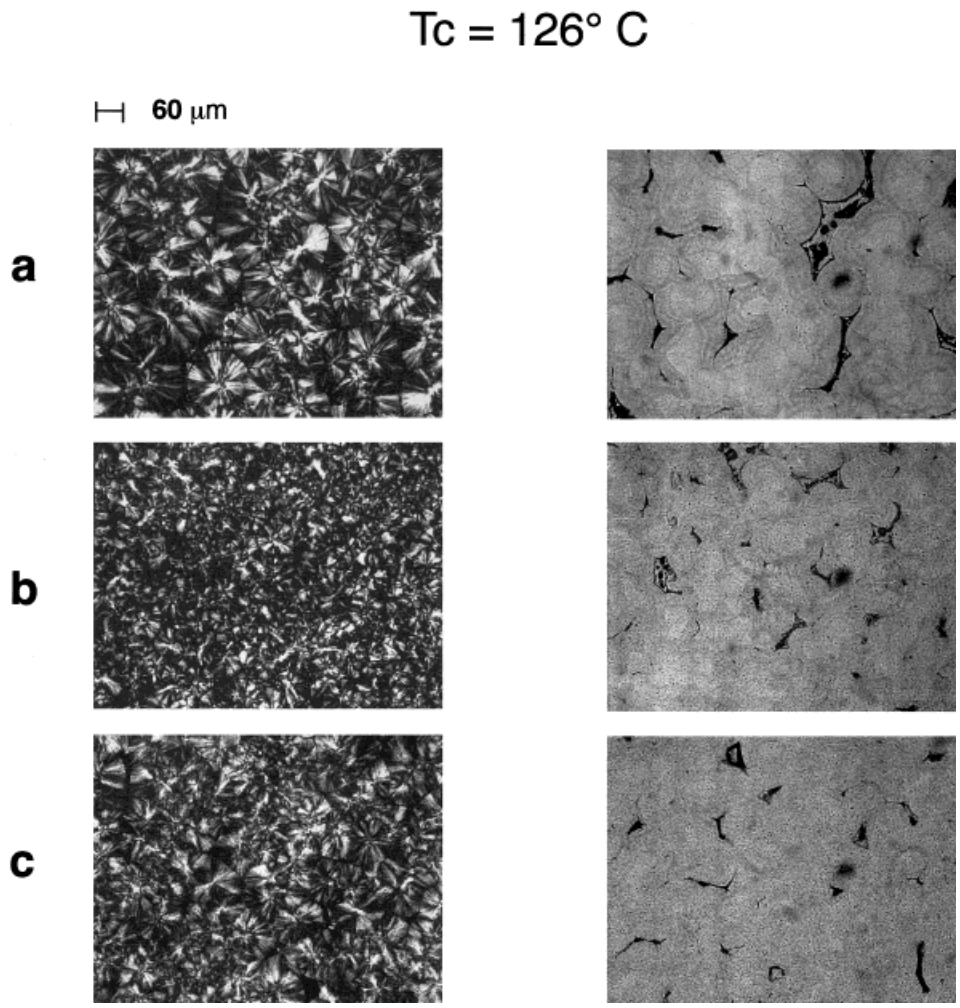

Figure 1 Optical micrographs taken at crossed and parallel polarizers of thin films of (a) (98:2) iPP/uPP-*g*-PS, (b) (95:5) iPP/uPP-*g*-PS, and (c) (90:10) iPP/uPP-*g*-PS blends isothermally crystallized at the temperature of 126°C.

$$X_c(\text{blend}) = \Delta H^*(\text{blend})/\Delta H^0(\text{iPP}) \qquad (2)$$

where ΔH^*(iPP) is the apparent enthalpy of fusion per gram of iPP in the blend; ΔH^o(iPP) is the heat of fusion per gram of 100% crystalline iPP, from 6 ΔH^o(iPP) = 209 J/g, and ΔH^*(blend) is the apparent enthalpy of fusion per gram of blend. The crystalline weight fractions referred to the iPP phase in blends [X_c(iPP)] were calculated from the following relation:

$$X_c(\text{iPP}) = X_c(\text{blend})/W(\text{iPP}) \qquad (3)$$

where W(iPP) is the weight fraction of iPP in the blends.

OM

Thin films of plain iPP and its blends isothermally crystallized at the temperatures of 126, 130, 134, and 138°C according to the same procedure used to study the isothermal crystallization process of the iPP phase by DSC, were observed by means of OM. A Zeiss optical polarizing microscope fitted with a Mettler hot stage was used; optical micrographs were taken with crossed and parallel polarizers. The radial growth rates (G) of the observed iPP spherulites were calculated by measuring the spherulite size (R) as a function of time; the photomicrographs were taken on the print and G was calculated as the slope of the straight lines obtained by plotting R against the

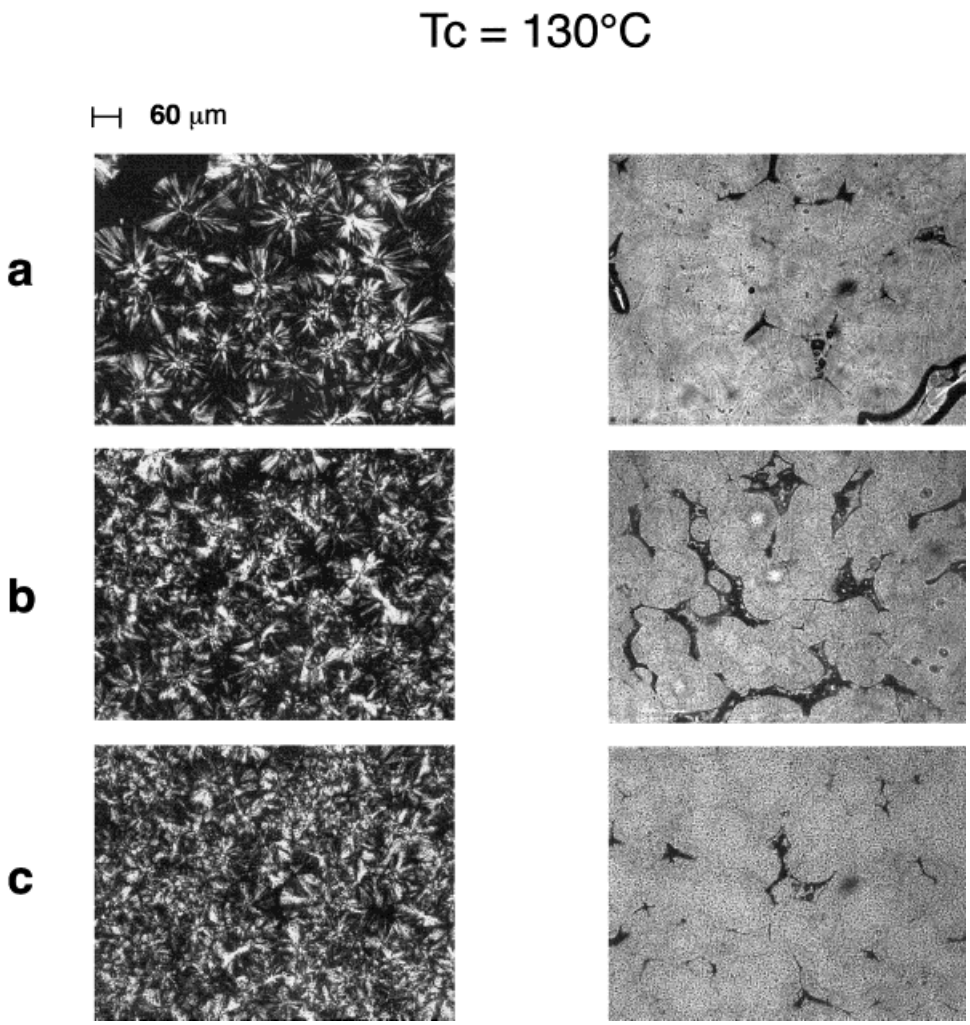

Figure 2 Optical micrographs taken at crossed and parallel polarizers of thin films of (a) (98:2) iPP/uPP-*g*-PS, (b) (95:5) iPP/uPP-*g*-PS, and (c) (90:10) iPP/uPP-*g*-PS blends isothermally crystallized at the temperature of 130°C.

time. The Zeiss microscope was also used to observe melts of binary and ternary blends at the temperature of 200°C and kept at this temperature for 10 min.

SAXS

SAXS studies on films of plain iPP and its blends isothermally crystallized at the temperatures of 126, 130, 134, and 138°C were performed by means of a compact Kratky camera equipped with a Braun one-dimensional positional sensitive detector. Ni-filtered CuKμ radiation generated from a Philips X-ray generator (PW 1730/10) operating at 40 KV and 30 mA, was used. The raw scattering data were corrected for parasitic scattering, absorption, and slit smearing by using Vonk's method.[7] The desmeared intensities were then Lorentz factor corrected by multiplying by s^2 ($s = 2 \sin\theta/\lambda$).[8]

RESULTS AND DISCUSSION

Microscopy Studies in Melt and Solid State

Optical micrographs, taken with parallel polarizers, of thin films of binary iPP/uPP-*g*-PS blends melted at the temperature of 200°C, and kept at this temperature for 10 min to destroy any crystallinity trace, have been reported in a previous article.[1] It is to be recalled that the iPP/uPP-*g*-PS

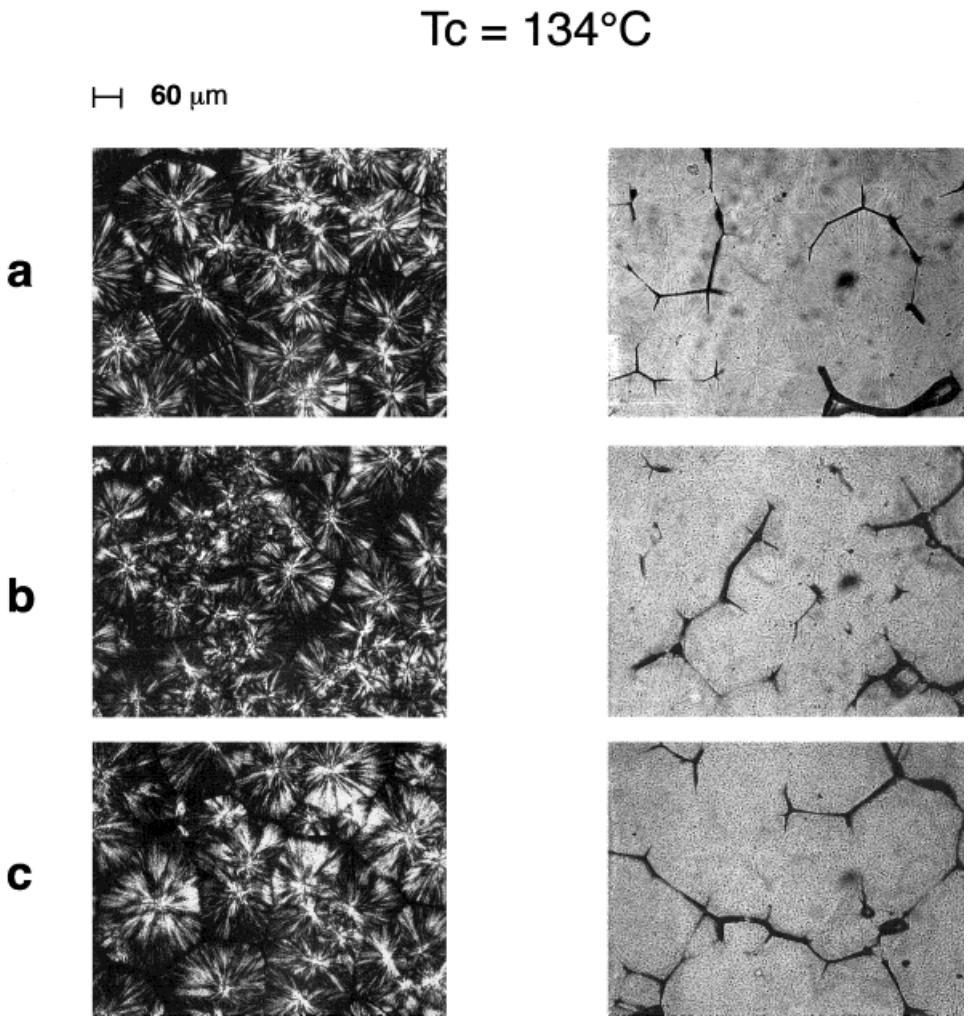

Figure 3 Optical micrographs taken at crossed and parallel polarizers of thin films of (a) (98:2) iPP/uPP-*g*-PS, (b) (95:5) iPP/uPP-*g*-PS, and (c) (90:10) iPP/uPP-*g*-PS blends isothermally crystallized at the temperature of 134°C.

melts exhibit phase separation with comparable fine dispersion degree of spherical-shaped domains of minor component, irrespective of copolymer content in the blends (wt/wt). By visual impression, in fact, the number of domains of the dispersed phase per unit area increase with increasing uPP-*g*-PS content. Such results suggest low interfacial tension between the iPP and uPP-*g*-PS copolymer and a mode of dispersion of minor component in the melt independent of composition; i.e., no coalescence phenomenon occurring by domains of dispersed phase with increasing copolymer content. The variation of tangent δ with temperature for such blends shows that, regardless of blend composition, a single T_g is found to be ascribed to the iPP phase; such T_g value can be considered within the experimental error to be the same T_g value as the plain iPP.[1] Therefore, the results so far obtained indicate immiscibility of the uPP-*g*-PS phase with iPP in the amorphous condensed state and iPP crystal growth starting from phase separated melts.

Optical micrographs, taken with crossed and parallel polarizers of thin films of iPP/ uPP-*g*-PS blends isothermally crystallized at 126, 130, 134, and 138°C, are reported in Figures 1–4; for comparison, optical micrographs taken with crossed and parallel polarizers of thin films of plain iPP at the investigated T_c are reported in Figure 5. As shown, the iPP/uPP-*g*-PS blends exhibit spherulitic superstructure with spherical-shaped domains of dispersed phase mainly occluded in the

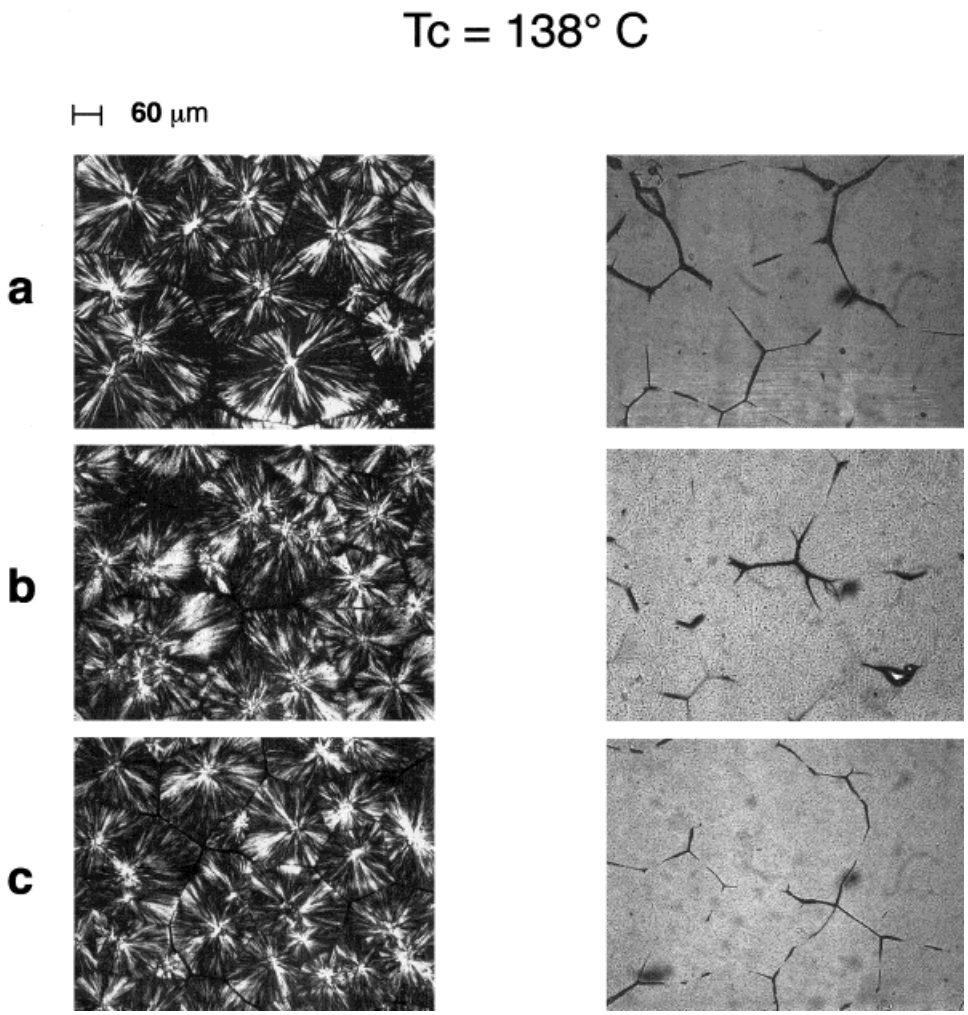

Figure 4 Optical micrographs taken at crossed and parallel polarizers of thin films of (a) (98:2) iPP/uPP-*g*-PS, (b) (95:5) iPP/uPP-*g*-PS, and (c) (90:10) iPP/uPP-*g*-PS blends isothermally crystallized at the temperature of 138°C.

iPP intraspherulitic regions rather than rejected by the crystallizing front at the boundary of the spherulites and in the interspherulitic contact regions. For a given composition, as expected, the iPP spherulites' size increases with increasing T_c (compare Figs. 1–4).

For a given T_c, it is to be noted that, surprisingly, the iPP spherulites crystallized in the presence of uPP-*g*-PS copolymer show size and regularity higher than that exhibited by the plain iPP with no systematic dependence on composition (compare Figs. 1–4 with Fig. 5). By comparing the spherulitic texture exhibited by the iPP/uPP-*g*-PS blends, for lower investigated T_c (126 and 130°C), it becomes apparent that spherulites with comparatively lower size and regularity are formed by the iPP phase crystallized in the presence of 5% uPP-*g*-PS copolymer, whereas larger and more regular spherulites are exhibited by the iPP phase crystallized from melts containing 2% copolymer (see Figs. 1 and 2). Such results suggest the occurrence of a migration phenomenon of heterogeneous nuclei from the iPP phase toward the uPP-*g*-PS phase, affecting the nucleation density of the iPP phase in the blends with no systematic dependence on composition. With increasing T_c, the extent of such a phenomenon becomes less pronounced (compare Figs. 1 and 2 with Figs. 3 and 4). Moreover, neither coalescence phenomenon is undergone by the primary particles formed in the melt state or the presence of irregular-

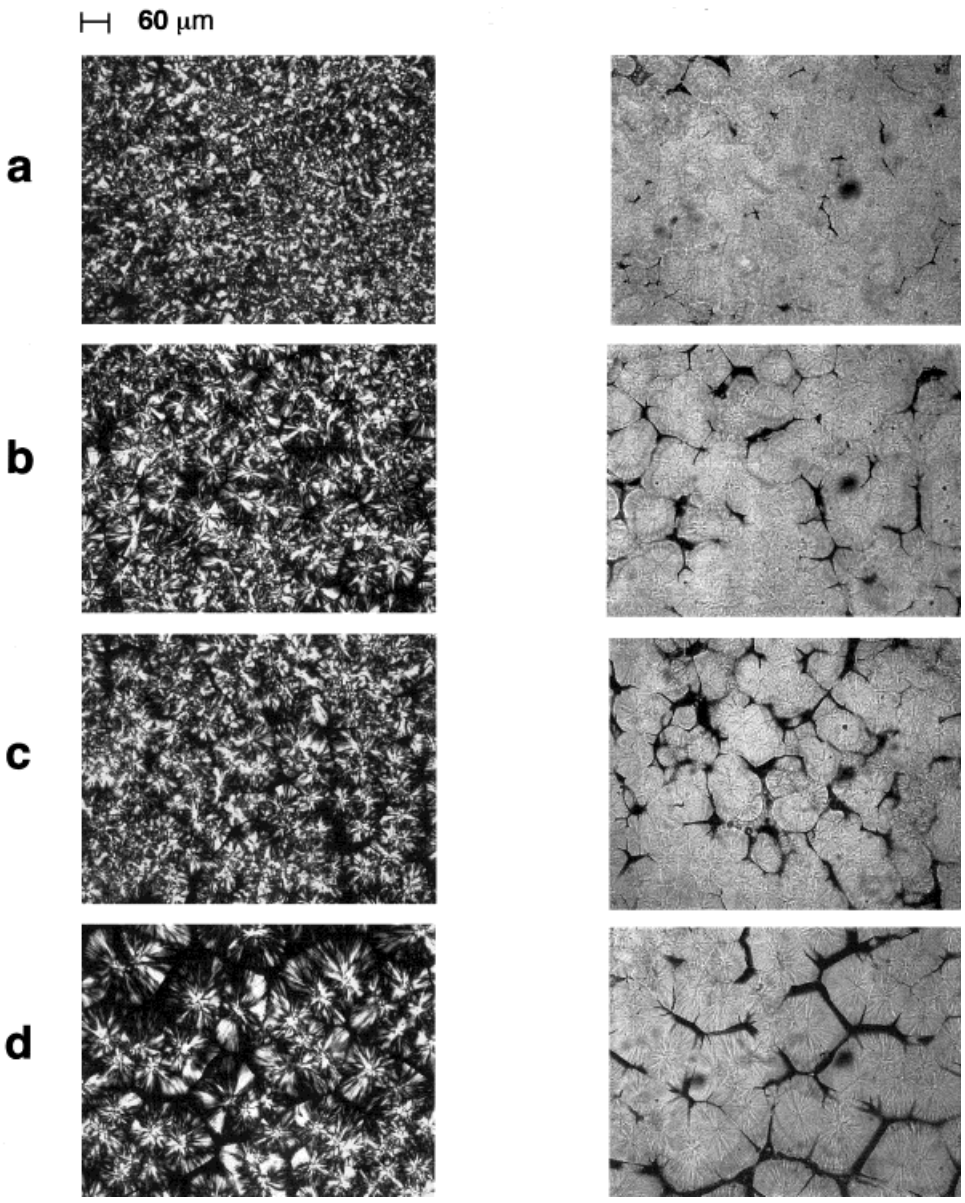

Figure 5 Optical micrographs taken at crossed and parallel polarizers of thin films of plain iPP isothermally crystallized at the temperatures of (a) 126°C, (b) 130°C, (c) 134°C, and (d) 138°C.

shaped domains, indicating deformation work performed by the spherulite growing front is observed.

It is to be pointed out that, when iPP crystallizes in the presence of the uPP-*g*-PS phase, the amount of amorphous material rejected in intraspherulitic contact regions, contrary to expectation, decreases with increasing T_c and, for a given T_c, with enhancing copolymer content (see Figs. 1–4). For higher investigated T_c, amorphous interspherulitic contact regions, smaller than that shown by the plain iPP, are developed (compare Figs. 3 and 4 with Fig. 5).

By comparing the mode and state of dispersion of the minor component in the solid state with that in the melt state it becomes apparent that, irrespective of the rate of the iPP crystallization at the examined T_c, the crystallization process of the iPP phase does not change the melt morphology of the dispersed phase.

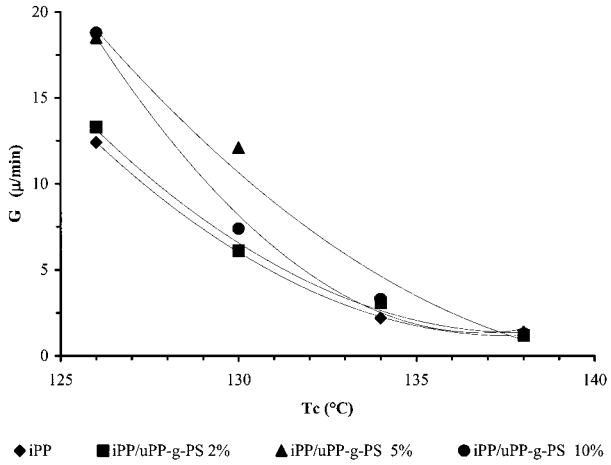

Figure 6 Plots of the radial grow rate (G) of iPP spherulites isothermally crystallized from melts of plain iPP and iPP/uPP-*g*-PS blends as a function of crystallization temperature (T_c).

Plots of the radius of iPP spherulites crystallized from melts of plain iPP and binary iPP/uPP-*g*-PS blends against time for all the crystallization temperatures investigated give straight lines indicating that, irrespective of composition, the concentration of propylenic crystallizable sequences at the growth front is constant during the crystallization process. For high undercooling, the values of the G of the iPP spherulites depends on blend composition, whereas with reducing undercooling, such values are almost constant, approaching those calculated for the plain iPP (see Fig. 6). In particular, for high undercooling, the plain iPP shows G values comparable to that shown by the iPP phase crystallized in the presence of 2% of the uPP-*g*-PS phase. The spherulites of the iPP phase grown from iPP/uPP-*g*-PS melts containing 5 and 10% of copolymer (wt/wt) show, at Tc equal to 126°C, G values significantly higher than that found for spherulites grown from binary melts containing lower uPP-*g*-PS content. Such findings could be accounted for by a comparatively lower molecular entanglements concentration influencing the activation free energy for the transport process through the liquid–solid interface (ΔF^*) according to the well-known Turnbull-Fisher equation[9] and/or by phenomenon of occlusion of dispersed domains by the growing spherulites according to Bartczak et al.[10] As far as the activation free energy for the transport process through the liquid–solid interface is concerned, it is moreover to be taken into account that the problem of the conversion to surface nucleation and lamellar growth, earlier treated by Turnbull and Fisher, requires consideration of a number of new features, such as accounting for the work of chain folding, the quite different nature of the transport mechanism (repetition) in the polymer melt, the effect of chain length, the segmental nature of the polymer chain, and questions related to the substrate length and the nature of a surface nucleus on a bladelike structure.[11] It could therefore be hypothesized that for high undercooling, the rate of transport of the iPP crystallizable sequences in the iPP/uPP-*g*-PS melts can be promoted according to a combination of thermodynamic and kinetic effects related to composition and mode and state of dispersion of minor component in the melt state.

DSC Studies

The thermograms of isothermally crystallized samples of plain iPP and its iPP/uPP-*g*-PS blends show, for all the investigated crystallization tem-

Table II Apparent Melting Temperatures (T'_m) for Plain iPP and iPP Crystallized from Its Blends as a Function of the Crystallization Temperature (T_c)

	T'_m (°C)			
Sample	T_c = 126°C	T_c = 130°C	T_c = 134°C	T_c = 138°C
iPP	164	166	169	171
iPP/uPP-*g*-PS 98/2 (wt/wt)	163	165	167	170
iPP/uPP-*g*-PS 95/5 (wt/wt)	161	163	164	167
iPP/uPP-*g*-PS 90/10 (wt/wt)	161	162	163	163

Table III Crystallinity Indices (X_c) of Plain iPP and iPP/uPP-*g*-PS Blends as a Function of the Crystallization Temperature (T_c)

	X_c			
Sample	T_c = 126°C	T_c = 130°C	T_c = 134°C	T_c = 138°C
iPP	0.50	0.52	0.53	0.54
iPP/uPP-*g*-PS 98/2 (wt/wt)	0.51	0.52	0.53	0.53
iPP/uPP-*g*-PS 95/5 (wt/wt)	0.51	0.52	0.53	0.52
iPP/uPP-*g*-PS 90/10 (wt/wt)	0.50	0.49	0.50	0.53

peratures, a single endothermic peak when heated from room temperature up to 200°C; the temperatures corresponding to the maxima of such peaks (T'_m) are reported in Table II. The crystallinity indices of the blends (X_c) and of the iPP phase [X_c(iPP)] for the T_c investigated are reported in Tables III and IV, respectively. As shown in Tables II– IV, and as expected, the apparent melting temperature values and crystallinity indices of all the investigated samples tend to increase with increasing crystallization temperature. For a given T_c, the following results are observed:

1. The T'_m values shown by the iPP phase crystallized in the presence of the uPP-*g*-PS phase are lower than that shown by the plain iPP; moreover, such values tend to decrease with increasing uPP-*g*-PS content. Note that the extent of such a decrease as a function of composition increases with increasing the *Tc* value (see Table II).
2. The crystallinity indices of the iPP/uPP-*g*-PS blends are almost comparable to that exhibited by the plain iPP with no systematic dependence on composition (see Table III).
3. The X_c values of the iPP phase crystallized from the iPP/uPP-*g*-PS blends are comparable or even higher than that shown by the plain iPP, indicating that the presence of the uPP-*g*-PS phase, irrespective of composition, does not come into opposition with the iPP crystallization process.

SAXS

Typical Lorentz-corrected desmeared patterns for isothermally crystallized samples of iPP/uPP-*g*-PS blends are shown in Figure 7. As shown, such SAXS profiles exhibit well-defined maxima: by applying Bragg's law, the long period (L) of the iPP phase has been calculated from the peak position. Assuming a two-phase model for the iPP

Table IV Crystallinity Indices of the iPP Phase as a Function of the Crystallization Temperature (T_c)

	$X_{c(\mathrm{iPP})}$			
Sample	T_c = 126°C	T_c = 130°C	T_c = 134°C	T_c = 138°C
iPP	0.50	0.52	0.53	0.54
iPP/uPP-*g*-PS 98/2 (wt/wt)	0.51	0.52	0.53	0.53
iPP/uPP-*g*-PS 95/5 (wt/wt)	0.52	0.53	0.54	0.53
iPP/uPP-*g*-PS 90/10 (wt/wt)	0.52	0.51	0.52	0.55

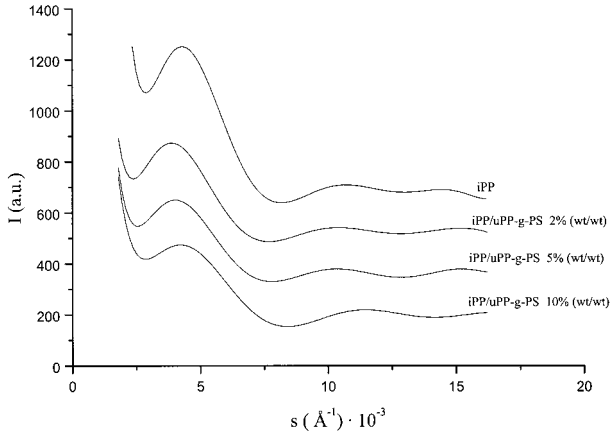

Figure 7 Typical SAXS Lorentz-corrected desmeared profiles for samples of iPP/uPP-*g*-PS blends isothermally crystallized at the temperature of 138°C.

spherulite fibrillae, consisting of alternating parallel crystalline lamellae and amorphous layers, the crystalline lamellar thickness (L_c) has been calculated using the following relation for the L values:

$$L_c = \frac{X_{c(\text{iPP})} \cdot L}{(\rho_c/\rho_a)(1 - X_{c(\text{iPP})} + X_{c(\text{iPP})}} \tag{4}$$

where $X_{c(\text{ipp})}$ is the DSC crystallinity index of the iPP phase and ρ_c and ρ_a are the densities of the crystalline and amorphous iPP phase, respectively. The thickness of the amorphous interlamellar layer (L_a) has been calculated by:

$$L_a = L - L_c \tag{5}$$

The long period, lamellar thickness, and amorphous interlamellar thickness of the plain iPP and iPP crystallized from iPP/uPP-*g*-PS blends are reported in Tables V–VII as a function of T_c. As to be expected for both plain iPP and iPP crystallized from its blends, L and L_c values increase with increasing crystallization temperature (see Tables V and VI). However, for a given T_c there is no clear dependence of the L values upon composition. It is interesting to observe that (for a given T_c) when iPP crystallizes in the presence of uPP-*g*-PS copolymer, the phase structure developed in the blends is characterized by crystalline lamellar thickness and interlamellar amorphous layer almost comparable, within the experimental error, to that respectively shown by plain iPP (see Tables VI and VII) with no dependence on composition. Such results agree with DSC results, confirming that the presence of the uPP-*g*-PS phase, irrespective of its content, does not come into opposition with the iPP crystallization process. Moreover, the finding that, irrespective of T_c, no significant increases in the L values are found, indicates that the uPP-*g*-PS phase is not present between the iPP lamellae.

By plotting the T'_m obtained by DSC versus the inverse of the crystalline lamellar thickness of the iPP phase ($1/L_c$) straight lines can be drawn (see Fig. 8). Thus, the trend of T'_m against L_c can be described by the following relation:

$$T'_m = T_m - \frac{2\sigma_e T_m}{\Delta H_f} \frac{1}{L_c} \tag{6}$$

where T'_m is the apparent melting temperature, ΔH_f the enthalpy of fusion of 100% crystalline

Table V The Long Period (L) Values for Plain iPP and iPP Crystallized from Its Blends as a Function of the Crystallization Temperature (T_c)

	L (Å)			
Sample	T_c = 126°C	T_c = 130°C	T_c = 134°C	T_c = 138°C
iPP	183	188	219	232
iPP/uPP-*g*-PS 98/2 (wt/wt)	181	195	200	243
iPP/uPP-*g*-PS 95/5 (wt/wt)	181	190	210	222
iPP/uPP-*g*-PS 90/10 (wt/wt)	166	190	216	216

Table VI Crystalline Lamella Thickness (L_c) Values for Plain iPP and iPP Crystallized from Its Blends as a Function of the Crystallization Temperature (T_c)

	L_c (Å)			
Sample	T_c = 126°C	T_c = 130°C	T_c = 134°C	T_c = 138°C
iPP	87	93	111	120
iPP/uPP-*g*-PS 98/2 (wt/wt)	88	97	101	123
iPP/uPP-*g*-PS 95/5 (wt/wt)	90	96	108	112
iPP/uPP-*g*-PS 90/10 (wt/wt)	82	92	107	114

iPP, L_c the crystalline lamellar thickness, T_m the equilibrium melting temperature, and σ_e the surface free energy of folding. According to this equation, T_m and σ_e can be respectively determined from the intercept and slope of the straight lines obtained by plotting T'_m against $1/L_c$. The T_m and σ_e values determined by this method are reported in Table VIII. As shown, the plain iPP shows T_m and σ_e values in line with those reported in the literature,[5] whereas the iPP phase crystallized in the presence of the uPP-*g*-PS phase shows both T_m and σ_e values strongly dependent upon composition, i.e., upon uPP-*g*-PS content. Note that the iPP phase crystallized in the presence of 2 and 5% of the uPP-*g*-PS phase shows T_m values comparable to that shown by the plain iPP and σ_e values slightly higher than that found for plain iPP. With increasing uPP-*g*-PS content, both T_m and σ_e values dramatically decrease (see Table VIII); lowered T_m value revealing, moreover, that for a given T_c, the iPP crystal growth, from melts containing 10% of the uPP-*g*-PS phase, occurred under comparatively lower undercooling. The folding surface free energy can be expressed by the fundamental thermodynamic equation[12]:

$$\sigma_e = \Delta H_e - TS_e \tag{7}$$

where ΔH_e is the folding surface enthalpy and S_e the folding surface entropy. The σ_e variation can be attributed to a variation of the S_e term. Therefore, the observed changes in σ_e values shown by the iPP crystals grown from iPP/uPP-*g*-PS melts are presumably due to changes in the S_e term; that is, to lower or higher surface disorder of lamellar crystals respectively related to a decrease or an increase of the presence of defects. In

Table VII Interlamellar Amorphous Layer Thickness (L_a) Values for Plain iPP and iPP Crystallized from Its Blends as a Function of the Crystallization Temperature (T_c)

	L_a (Å)			
Sample	T_c = 126°C	T_c = 130°C	T_c = 134°C	T_c = 138°C
iPP	96	95	108	112
iPP/uPP-*g*-PS 98/2 (wt/wt)	93	98	99	120
iPP/uPP-*g*-PS 95/5 (wt/wt)	91	94	102	110
iPP/uPP-*g*-PS 90/10 (wt/wt)	84	98	109	102

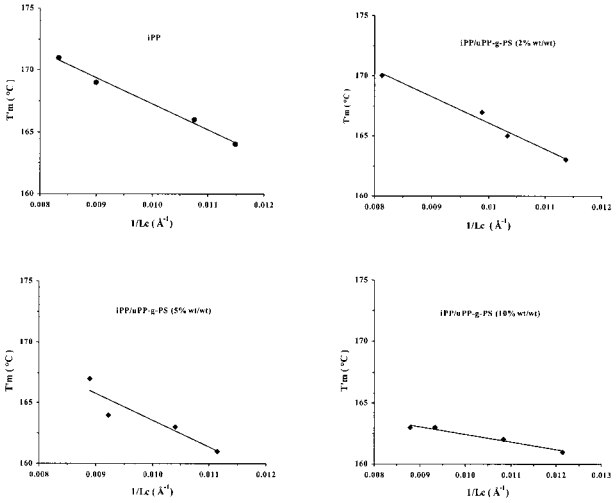

Figure 8 Plots of the apparent melting temperatures (T'_m) versus the inverse of lamellar thickness ($1/L_c$) of the iPP phase isothermally crystallized from melts of plain iPP and iPP/uPP-*g*-PS blends.

other words, the obtained results display that iPP crystals grown in the presence of the uPP-*g*-PS phase can be characterized, according to composition, by surfaces more or noticeably less regular and unperturbed than that exhibited by plain iPP.

Considering all the above results, the lamellar structure of the iPP phase developed in the investigated iPP/uPP-*g*-PS blends is compared with that generated in plain iPP according to the schematic models reported in Figure 9.

CONCLUSION

Samples of blends of iPP and uPP-*g*-PS isothermally crystallized from melt at the temperatures of 126, 130, 134, and 138°C show spherulitic superstructure with spherical-shaped domains of dispersed phase mainly occluded in the iPP intraspherulitic regions—the number of such domains increasing with increasing copolymer content. By comparing modes and states of dispersion of minor component in the melt state with that developed after iPP complete crystallization, it was found that the crystallization process does not change the very fine dispersion degree of minor component achieved in the melt state, irrespective of both composition and rate of the iPP crystallization at the examined T_c.

For a given T_c, the iPP spherulites crystallized in the presence of uPP-*g*-PS copolymer surprisingly show size and regularity higher than that exhibited by the spherulites of plain iPP with no systematic dependence on composition. Moreover, the amount of amorphous material rejected in intraspherulitic contact regions decreases with increasing T_c and, for a given T_c, with enhancing copolymer content. Assuming a two-phase model for the iPP spherulitae fibrillae, consisting of alternating parallel crystalline lamellae and amorphous layers, the lamellar structure of the iPP phase in the blends is characterized by crystalline lamellar thickness and interlamellar amorphous layer thickness comparable to that shown by plain iPP. The T'_m values shown by the iPP phase crystallized in presence of the uPP-*g*-PS phase are lower than that exhibited by the plain iPP and decrease with increasing uPP-*g*-PS content. However, the crystallinity indices of the iPP phase crystallized from binary melts, irrespective of composition, are comparable to that shown by the plain iPP, indicating that the presence of uPP-*g*-PS copolymer does not come into opposition with the iPP crystallization process. These morphological and structural evidences could be accounted for by assuming that the iPP crystallization process could occur through molecular fractionation and thus iPP molecules with low constitutional and configurational regularity could be dissolved in domains more rich in uncrystallizable uPP-*g*-PS component. Also, relevant thermodynamic parameters of the resultant iPP phase were strongly affected by the presence of the uPP-*g*-PS phase, although opposite effects were observed depending on copolymer content. For uPP-*g*-PS content up to 5 %, the values of the equilibrium melting temperature (T_m) and of the superficial free energy of folding (σ_e) of the iPP phase are respectively slightly lower and higher

Table VIII Equilibrium Melting Temperature (T_m) and Surface Free Energy of Folding (σ_e) Values of Plain iPP and iPP Phase Crystallized from Its Blends

Sample	T_m (°C)	σ_e (erg/cm^2)
iPP	189	118
iPP/uPP-*g*-PS 98/2 (wt/wt)	188	122
iPP/uPP-*g*-PS 95/5 (wt/wt)	186	125
iPP/uPP-*g*-PS 90/10 (wt/wt)	169	39

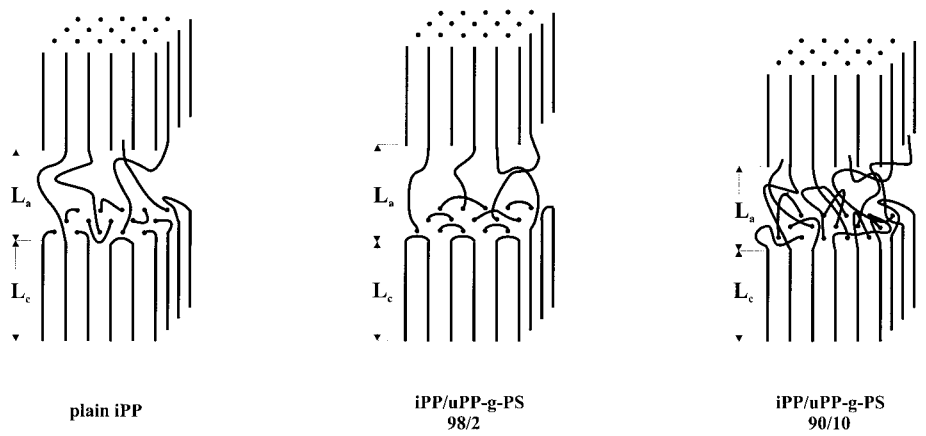

Figure 9 Schematic models of the lamellar structure of the iPP phase crystallized under controlled undercooling from melts of plain iPP and iPP/uPP-*g*-PS blends.

than that found for the plain iPP. By further increase of copolymer content, both T_m and σ_e values decrease dramatically. Such findings could be presumably ascribed to a combination of morphological and thermodynamic effects, likely induced by an iPP fractionated crystallization process, related to mode and state of dispersion of minor component and to miscibility in the melt state, respectively.

Work is in progress to investigate phase and inter-phase morphology developed in samples of iPP/uPP-*g*-PS melts annealed at low undercooling values.

REFERENCES

1. D'Orazio, L.; Guarino, R.; Mancarella, C.; Martuscelli, E. J Appl Polym Sci 2000, 75, 553.
2. D'Orazio, L.; Guarino, R.; Mancarella, C.; Martuscelli, E. J Appl Polym Sci 1997, 65, 1539.
3. D'Orazio, L.; Guarino, R.; Mancarella, C.; Martuscelli, E. J Appl Polym Sci 1999, 72, 1429.
4. Cecchin, G.; Guglielmi, F.; Zerega, F. U. S. Pat. 4,602,077, 1986.
5. Cecchin, G.; De Nicola, A. U. S. Pat. 5,159,023, 1990.
6. Brandrup, S.; Immergut, E. M. Polymer Handbook; Interscience: New York, 1975; Vol. 5.
7. Vonk, C. G. J Appl Crystallogr 1975, 8, 340.
8. Alexander, L. E. X-Ray Diffraction in Polymer Science; Wiley: New York, 1969.
9. Turnbull, D.; Fisher, J. C. J Chem Phys 1949, 17, 71.
10. Bartczak, Z.; Galeski, A.; Martuscelli, E. Polym Eng Sci 1984, 24, 1155.
11. Hoffman, J. D.; Miller, R. L. Polymer 1997, 38, 3151.
12. Wunderlich B. Macromolecular Physics; Academic Press: New York, 1976.